



HAL
open science

Analytical methods of antibody surface coverage and orientation on bio-functionalized magnetic beads: application to immunocapture of TNF- α

Etienne Laborie, Victor Le-Minh, Thanh Duc Mai, Mehdi Ammar, Myriam Taverna, Claire Smadja

► To cite this version:

Etienne Laborie, Victor Le-Minh, Thanh Duc Mai, Mehdi Ammar, Myriam Taverna, et al.. Analytical methods of antibody surface coverage and orientation on bio-functionalized magnetic beads: application to immunocapture of TNF- α . *Analytical and Bioanalytical Chemistry*, 2021, 413 (25), pp.6425-6434. <10.1007/s00216-021-03608-w>. <hal-03840228>

HAL Id: hal-03840228

<https://universite-paris-saclay.hal.science/hal-03840228v1>

Submitted on 15 May 2023

HAL is a multi-disciplinary open access archive for the deposit and dissemination of scientific research documents, whether they are published or not. The documents may come from teaching and research institutions in France or abroad, or from public or private research centers.

L'archive ouverte pluridisciplinaire HAL, est destinée au dépôt et à la diffusion de documents scientifiques de niveau recherche, publiés ou non, émanant des établissements d'enseignement et de recherche français ou étrangers, des laboratoires publics ou privés.



HAL Authorization

1 **gAnalytical methods of antibody surface coverage and orientation on bio-functionalized**
2 **magnetic beads: application to immunocapture of TNF- α**

3

4 **Etienne Laborie^{1,2}, Victor Le-Minh¹, Thanh Duc Mai¹, Mehdi Ammar², Myriam**
5 **Taverna^{1,3}, Claire Smadja¹**

6

7 *¹ Université Paris-Saclay, CNRS, Institut Galien Paris-Saclay, Protein and Nanotechnology*
8 *in Analytical Science, 92296, Châtenay-Malabry, France*

9 *² Université Paris-Saclay, CNRS, Centre de Nanosciences et de Nanotechnologies, 91120,*
10 *Palaiseau, France.*

11 *³ Institut Universitaire de France, France*

12

13

14 ✉ claire.smadja@universite-paris-saclay.fr

15

16 **Keywords:** magnetic beads, antibody; orientation, immunocapture; TNF- α ; immunoassays

17 **List of abbreviations**

18 COOH (carboxyl), EDC (N-(3-Dimethylaminopropyl)-N'-ethylcarbodiimide hydrochloride),

19 FLD (Fluorescent Detection), hIgG (human immunoglobulin G), PBS (Phosphate Buffer

20 Saline), SEC (Size Exclusion Chromatography), Sulfo-NHS (N-Hydroxysulfosuccinimide

21 sodium salt), TBS (Tris Buffer Saline), Ts (Tosyl),

22

23

24

25 **Author contributions**

26 **Etienne Laborie**: Investigation, writing original draft, validation, **Victor Le-Minh**:
27 investigation, writing-review, **Thanh Duc Mai**: writing original draft, **Mehdi Ammar**:
28 resources, supervision, **Myriam Taverna**: resources, writing-review, **Claire Smadja**:
29 funding, project supervision, writing –original draft.

30
31 **Conflicts of interest/Competing interests**

32 The authors have no conflicts of interest to declare that are relevant to the content of this article.

33
34 **Acknowledgements**

35 We thank the “Investissement d’Avenir” program, through the “IDI 2017” project funded by
36 the IDEX Paris-Saclay, ANR-11-IDEX-0003-02 which provided the financial support of
37 Etienne Laborie as a fellowship, LabeX LaSIPS (ANR-10-LABX-0040-LaSIPS) and LabeX
38 NanoSaclay, (ANR-10-LABX-0035).

39 We thank the Doctoral school of Chemical Sciences of University Paris Saclay which provided
40 the financial support of Victor Le-Minh as a fellowship

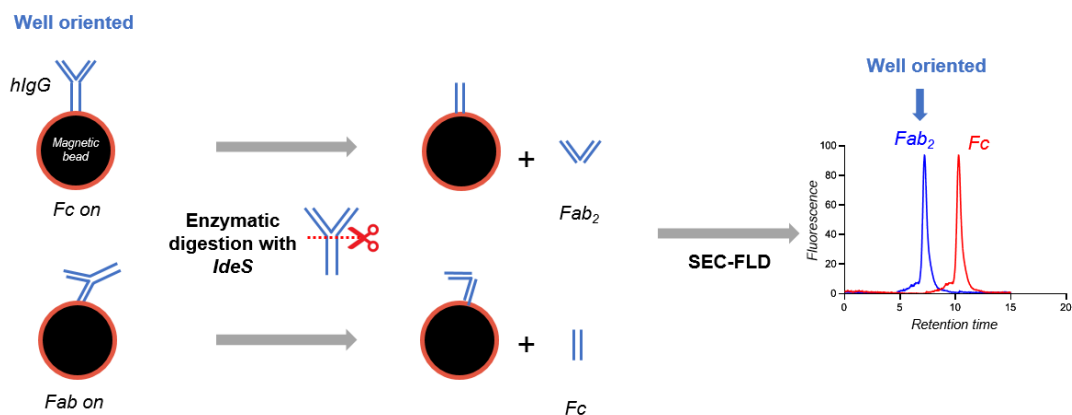
41
42 **Availability of data and material** Not applicable

43
44 **Code availability** Not applicable

45
46
47 **Graphical Abstract**

48 A rapid and simple approach to evaluate orientation and density of antibodies immobilized on
49 magnetic beads

50



51

52

53

54

55

56

57

58 **Abstract**

59
60 The use of magnetic beads bio-functionalized by antibodies (Ab), is constantly increasing with
61 a wide range of biomedical applications. However, despite an urgent need for current methods
62 to monitor Ab's grafting process and orientation, existing methods are still either cumbersome
63 and/or limited.

64 In this work, we propose a new simple and rapid analytical approach to evaluate antibody
65 orientation and density on magnetic beads. This approach relies on the cleavage by *IdeS*, a
66 highly specific protease for human immunoglobulin G (hIgG), of immobilized antibodies. The
67 F(ab)₂ and Fc fragments could be then accurately quantified by Size Exclusion Chromatography
68 (SEC)- coupled to fluorescent detection (FLD) and the ratio of these fragments was used to give
69 insight on the IgG orientation at the bead surface. Four different commercially available
70 magnetic beads, bearing carboxyl groups, tosyl groups, streptavidin or protein G on their surface
71 have been used in this study. Results obtained showed that this approach ensures reliable
72 information on hIgG orientation and beads surface coverage. Protein G magnetic beads
73 demonstrated an optimal orientation of antibodies for antigen capture (75% of accessible Fab₂
74 fragment) compared to tosylactivated, carboxylated and streptavidin ones. Capture efficiency
75 of the different functionalized beads toward human TNF- α immunocapture, a biomarker of
76 inflammation, has been also compared. Protein G beads provided a more efficient capture
77 compared to other beads. In the future, this approach could be applied to any type of surface
78 and beads to assess ~~the~~ hIgG coverage and orientation after any type of immobilization.

79

80

81

82

83

84

85 **1. Introduction**

86 Magnetic beads with their several advantages have found increasing applications in many fields
87 including drug discovery, biomedicine, bioassays, diagnostics, genomics and proteomics [1, 2].

88 A typical application is peptides/proteins selective capture *via* magnetic separation using
89 magnetic beads functionalized with a bio-receptor. Many recently developed diagnostic tools
90 (e.g. lab-on-a-chip and biosensors) are based on bio-functionalized magnetic particles with
91 antibodies [3]. For these purposes, several types of magnetic beads are currently available
92 differing by their sizes, shape, surface chemistry and immobilization strategy that are crucial
93 for antibodies grafting density and orientation. Preparation of magnetic nanoparticles with a
94 stable surface remains of paramount importance. After the coating step bioreceptors such as
95 antibodies will biofunctionalized the nanoparticles to target specific biomarkers for instance. A
96 high antibody grafting density and a good orientation, which requires exposed and fully
97 available F(ab)₂ fragments on bead surface, are highly desirable to ensure high loading/capture
98 of target analytes during the immuno-precipitation/enrichment or bioassay processes.

99 The monitoring of surface antibody density and orientation is therefore critical not only for
100 capture or recognition efficiency but also to produce batches of functionalized magnetic beads
101 of equal performance and quality.

102 Conventional methods to assess the antibody immobilization on beads are based either on
103 spectrophotometric or biophysical methods. Colorimetric assays (e.g. Lowry, Bradford and
104 BCA assays) have been shown to provide only indirect determination of protein grafting
105 efficiency as they are mainly based on the determination of non- immobilized proteins present
106 in the supernatant [4][5]. In addition, they do not provide any information on antibodies
107 orientation. Besides, many biases have been reported with these methods mainly related to
108 possible background interferences due to nanoparticles themselves [6–8]. Atomic force

109 microscopy, surface plasmon resonance (SPR), spectroscopic ellipsometry and dual
110 polarization interferometry [5, 9–12] can provide indirect insight on antibodies orientation
111 mainly by measuring antibodies dimensions/thickness on surfaces or shift angle. Recently,
112 Lämmerhofer *et al.* proposed an approach for quantification of the protein surface coverage on
113 gold nanoparticles using high performance liquid chromatography (HPLC) [4, 13]. In this work,
114 pepsin conjugated to gold nanoparticles is hydrolyzed (6N HCl). The released amino acids are
115 tagged with a fluorescent dye and then analyzed by HPLC with fluorescence detection. The
116 derivatized Glycine measurement is used to estimate the pepsin surface coverage on
117 nanoparticles. Kozłowski *et al.* gave an estimate of surface coverage of dihydrofolate reductase
118 (DHFR)-gold particle bioconjugates, using a combination of several techniques including SDS-
119 PAGE, UV-vis spectrophotometry, dynamic light scattering and a fluorescence-based method
120 [6]. These methodologies allowed a fine protein surface coverage characterization but required
121 several steps and a combination of several techniques. In another study relying on streptavidin-
122 magnetic beads, Gagey-Eilstein *et al.* communicated a chemiluminescent test to monitor the
123 antibody grafting rate [14] and by sandwich-type immunoassay using magnetic beads grafted
124 with antibodies have been also reported [15, 16]. All these methods, however, did not provide
125 information on the antibody-grafting orientation nor on the functionality and ability of
126 antibodies to capture the biological target.

127
128 Herein we report the development of a method for quantification of antibody surface coverage
129 and monitoring of antibody grafting orientation on magnetic beads functionalized with different
130 functional groups or chemistries. Together with a recent publication by Shen *et al* [17], our
131 study is one of the two pioneering works which shed light on both orientation and density of
132 antibodies decorated on magnetic beads using chromatographic approaches. Shen *et al*
133 proposed a method which used a proteolysis performed by trypsin-decorated magnetic beads to

134 quantify the number of antibodies attached to magnetic beads. LC-MS/MS of the released
135 tryptic peptides allowed to quantify representative peptides of either the F(ab)₂ or Fc region of
136 the antibody. However, it is important to note that the release of F(ab)₂ peptides from antibodies
137 could arise from antibodies attached via one Fab fragment leading thereby to an overestimation
138 of the number of well oriented antibodies.

139 Our work relies on the use of a selective proteolysis of F(ab)₂ regions of antibodies, using (*IdeS*)
140 that cleaves antibodies with a unique degree of specificity in the hinge region leading to the
141 release of Fc and F(ab)₂ fragments [18]. Our straightforward analytical approach relied on size
142 exclusion liquid chromatography coupled to fluorescent detection (FLD) allowing F(ab)₂ and
143 Fc separation according to their molecular weight (100 and 50 kDa respectively) [17]. F(ab)₂
144 and Fc will be clearly identified with this new approach. In our case the quantification of the
145 ratio Fab / Fc is expected to be directly related to the orientation of immobilized antibodies.
146 Indeed, after *IdeS* digestion, if the antibodies are grafted through their Fc fragment, F(ab)₂ is
147 released whereas when they are immobilized via Fab fragment, Fc fragment is released. The
148 relevance and utility of the developed approach was demonstrated with a high diagnostic-value
149 application, by quantifying the human Tumor Necrosis Factor alpha (TNF- α), a pro-
150 inflammatory cytokine, serving for screening of Major Depressive Disorders (MDD) and which
151 is involved in many inflammatory disorders such as cytokine release syndrome observed in
152 COVID 19 [19–25].

153

154

155

156 **2. Experimental**

157 ***2.1. Chemicals and reagents***

158 *IdeS* FabRICATOR enzyme (5000 units) was purchased from Genovis AB (Lund, Sweden).
159 HPLC-grade propan-2-ol and sodium di-hydrogen phosphate (NaH₂PO₄) were obtained from
160 Fisher Scientific (Karlsruhe, Germany). Sodium chloride was provided from Euromedex
161 (Souffelweyersheim, France). 32% sodium hydroxide was purchased from VWR SAS
162 (Fontenay-sous-Bois, France). 85% phosphoric acid was obtained from Carlo Erba Reagents
163 (Val-de-Reuil, France). EZ-Link Sulfo-NHS-LC-biotin kit and Dynabeads MyOne
164 Carboxylated, Tosylactivated, Streptavidin T1, Pierce Protein G (1 μ m) magnetic beads and
165 TNF alpha Human Uncoated ELISA Kit were purchased from Life Technologies SAS
166 (Villebon-sur-Yvette, France). Human IgG from whole serum (10.2 mg/mL) and Amicon Ultra
167 0.5mL 50 kDa and 100 kDa filters for ultrafiltration were provided by Merck Millipore
168 (Darmstadt, Germany). Phosphate buffer saline 10X (PBS), Tris-buffer saline 10X (TBS), boric
169 acid, Tween 20, ammonium sulphate, N-(3-Dimethylaminopropyl)-N'-ethylcarbodiimide
170 hydrochloride (EDC) and N-Hydroxysulfosuccinimide sodium salt (Sulfo-NHS) were
171 purchased from Sigma Aldrich (St. Louis, MO, USA).

172

173 **2.2. Apparatus and Material**

174 Size exclusion liquid chromatography experiments were performed using an Agilent 1260
175 UHPLC- 1260 FLD detector (Xenon lamp) (Agilent Technologies, Santa Clara, CA, USA). An
176 Agilent Bio SEC-3 column (3 μ m particle size; 300 \AA pore structure; 300 mm length; 4.6 mm
177 i.d.) was employed at temperature of 25 $^{\circ}$ C. The mobile phase (50 mM sodium phosphate, 150
178 mM NaCl and 10% isopropanol at pH 6.5) was isocratically pumped at 300 μ L/min.
179 Fluorescence detection (FLD) was performed at $\lambda_{\text{ex}} = 280$ nm and $\lambda_{\text{em}} = 340$ nm. Data
180 acquisition and instrument control were performed by Chemstation (Agilent).

181

182 **2.3. Methods**

183 **2.3.1: Preparation of bio-functionalized magnetic beads**

184 Model human IgG (hIgG) were grafted on beads following commercial protocols for
185 streptavidin and protein G beads. For beads tosylactivated (Ts) and COOH the protocols have
186 been adapted from the supplier ones). IgG concentration in the grafting solution was kept
187 constant at 0.1 mg/mL for accurate comparison of beads grafting efficiency.

188

189 *2.3.1.1: Carboxylated magnetic beads*

190 100 μ L of Dynabeads MyOne Carboxylated (10 mg/mL) were added to 4 LoBind Eppendorf
191 vials of 1.5 mL and washed with 1 mL of 20 mM NaOH overnight on a rotating wheel (Tube
192 rotator SB3, Stuart, UK) at 20 rpm and 4°C. Beads were then concentrated using a magnet and
193 washed 3 times with 500 μ L of PBS. Then, beads were resuspended in 120 μ L of human IgG
194 solution at 0.66 mg/mL in PBS. 200 μ L of EDC (10 mg/mL) and 200 μ L of Sulfo-NHS (10
195 mg/mL) in PBS were added to the beads suspension. Finally, volume was adjusted to 800 μ L
196 with PBS, reaching a final concentration of 0.1 mg/mL of IgG for 1 mg of beads. Vials were
197 then placed on a rotating wheel at 20 rpm overnight at 4°C for antibody grafting and beads were
198 immobilized on a magnet and washed 2 times with 500 μ L of a solution of PBS, Tween 20
199 (0.05%) (PBS-Tween) and one time with 500 μ L of PBS. Washing solutions were kept at 4°C
200 until analysis.

201

202 *2.3.1.2: Tosylactivated magnetic beads*

203 10 μ L of Dynabeads MyOne Tosylactivated (100 mg/mL) were added to 4 LoBind Eppendorf
204 vials of 1.5 mL and washed with 500 μ L of 0.1 M sodium borate buffer pH 9.5, gently vortexed
205 and stirred at the same time using an Eppendorf Thermomixer for 15 min C at 25°C and 650
206 rpm. Beads were resuspended in 60 μ L of hIgG solution at 0.66 mg/mL in PBS with 60 μ L of
207 3M ammonium borate buffer pH 9.5 and 20 μ L of 0.1M sodium borate buffer. Vials containing

208 beads were then incubated at 37°C and stirred at 650 rpm on a Thermomixer for 16h and then
209 sonicated for 5 minutes to prevent their adsorption on the vial's walls. Beads ~~are~~ were
210 immobilized on a magnet and washed 2 times with 500 µL of a solution of PBS-Tween, and
211 one time with 500 µL of PBS. Washing solutions were kept at 4°C until their analysis.

212

213 *2.3.1.3: Streptavidin magnetic beads*

214 Biotinylation of human IgG was done using EZ-link sulfo-NHS-LC-biotin kit. A 10 mM
215 solution of biotin was prepared by adding 224µL of ultrapure water to 1 mg of biotin. 6.66 µL
216 of biotin solution was added to 1000 µL of hIgG solution (0.5 mg/mL) and incubated at 25°C
217 for 30 minutes and stirred at 300 rpm on a Thermomixer at the same time. The solution was
218 then ultrafiltrated on a 50 kDa filter cap at 4°C, 10 000 rpm for 4 minutes to get rid of biotin
219 salts excess.

220 100µL of Dynabeads MyOne Streptavidin T1 (10 mg/mL) are added to 4 LoBind Eppendorf
221 vials of 1.5 mL and washed with 1 mL of PBS-Tween solution. Beads ~~were~~ then immobilized
222 on a magnet and washed 3 times with 500 µL of PBS-Tween. ~~Beads were then resuspended in~~
223 ~~40 µL~~ of biotinylated hIgG solution at 0.5mg/mL ~~and~~ 160 µL of PBS. Vials ~~are~~ ~~were~~ then
224 incubated at 25°C, 450 rpm for 30 minutes on a Thermomixer and beads ~~are~~ ~~were~~ immobilized
225 on a magnet and supernatants are collected and kept at 4°C. Beads ~~were~~ washed 4 times with
226 500 µL of a solution of PBS Tween Washing solutions ~~were~~ kept at 4°C.

227

228 *2.3.1.4: Protein G magnetic beads*

229 100µL of Pierce Protein G Magnetic Beads (10 mg/mL) were added to 4 LoBind Eppendorf
230 vials of 1.5 mL and washed with 500 µL of Tris-Tween solution and gently vortexed. The
231 process was repeated one time with 1 mL of Tris-Tween. Beads were resuspended in 217 µL of
232 human IgG solution at 0.23 mg/mL with 283 µL of Tris-Tween. Vials were then incubated at

233 25°C, 650 rpm for 1 hour on a Thermomixer and beads were immobilized on a magnet and
234 supernatants were collected and kept in the fridge for analysis. Beads were then washed 2 times
235 with 500 µL with Tris-Tween. Washing solutions were kept in the fridge for analysis.

236

237 ***2.3.2 Characterization of the hIgG grafting***

238 *2.3.2.1 Enzymatic digestion of grafted antibodies*

239 For all digestions, 2µL aliquot of 100 U of *IdeS* FabRICATOR enzyme and 50 µL of phosphate
240 buffer (100 mM, pH 7.0) were added to the sample, hIgG solution (60 µL) or hIgG grafted on
241 magnetic beads (suspended) and incubated for 1h30 at 37°C 300 rpm on a Thermomixer. Beads
242 suspensions were then placed on a magnet and supernatants were collected and analyzed.

243

244 *2.3.2.2 Influence of beads grafting conditions on FLD signal for hIgG, F(ab)₂ and Fc fragments*

245 To avoid any bias in the measurements, the influence of beads grafting protocols (medium,
246 incubation steps) on hIgG FLD signals was investigated. Each sample was prepared in
247 duplicate. hIgG samples at 0.1 mg/mL were incubated following conjugation protocols
248 corresponding to tosylactivated carboxylic and protein G beads and then analyzed by SEC-
249 FLD.

250

251 *2.3.2.3 Calibration curves*

252 *hIgG*

253 Calibration curve for whole hIgG was obtained with a 0.1 mg/mL hIgG solution in PBS.
254 Dilution series of hIgG, ranging from 0.05 µg to 0.7 µg, have been injected analyzed to establish
255 the calibration curve.

256

257 *hIgG fragments*

258 Calibration samples were made from IgG stock solution submitted to the different conjugation's
259 protocols. hIgG solutions (0.23 mg/mL) were digested with 100 U of *IdeS* and analyzed with
260 by SEC-FLD. Volumes of hIgG digests from 0.5 μ L to 7 μ L were analyzed and a calibration
261 curve per conjugation protocol has been built for the two fragments (F(ab)₂ and Fc).

262

263 2.3.2.4: *Quantitation of non-grafted hIgG in the supernatant*

264 Antibodies remaining in the supernatant after the grafting step were first quantified. Then,
265 washing solutions were concentrated by ultrafiltration on 100 kDa membrane. 500 μ L of
266 washing solution was added to the filter cap and centrifuge for 4 minutes at 10 000 rpm at 4°C
267 on a Centrifuge MicroStar 17R (VWR). The process was repeated until all the solution was
268 filtered. Retentates volumes were measured before SEC-FLD analysis.

269

270 **2.3.3 Immuno-capture of TNF- α by biofunctionalized magnetic beads**

271 1 mg of COOH, Ts and Protein G magnetic beads were grafted with anti-human-TNF- α
272 monoclonal antibodies from the Invitrogen ELISA kit for human TNF- α following the
273 procedure described previously. Five replicates of 100 μ g of grafted magnetic beads of each
274 type were then incubated for 4 hours at 25°C with 5 ng of human TNF- α in 250 μ L of PBS (1X).
275 Three blank samples were also prepared using grafted magnetic beads and PBS (1X). Beads
276 were washed with 500 μ L of PBS-Tween for 10 minutes at 800 rpm on a Thermomixer. Then,
277 heated 95°C for 5 minutes in 250 μ L of PBS (1X) for thermal elution of TNF- α . Eluates were
278 diluted on PBS (1X, 10X, 100X) to match immunoassay detection range. Human TNF- α
279 contents of non-diluted and diluted eluates were quantified using Invitrogen ELISA kit for
280 human TNF- α using duplicates. Calibration curves were built by preparing serial dilution of
281 human TNF- α solution at 500 pg/mL with and without thermal treatment at 95°C for 5 minutes
282 to take into account the thermal effect on TNF- α .

283

284 **3. Results and Discussion**

285 The first part of the study was dedicated to the development of an analytical method to evaluate
286 the grafting efficiency on four types of beads. Two main criteria have been considered: number
287 of antibodies grafted on the bead's surface and their orientation. For this purpose, we
288 specifically cleaved ~~human~~-hIgG grafted on the beads surface under the hinge region with an
289 enzyme, *IdeS*, and analyzed the digestion products by SEC-FLD analysis. If the hIgG is
290 immobilized *via* its Fc region, the F(ab)₂ fragment will be released in the supernatant whereas
291 for immobilization through F(ab)₂ fragment, Fc fragment will be obtained.

292

293 **3.1. Influence of the grafting conditions on native and digested human IgG fluorescent** 294 **detection**

295 We first developed a SEC-Fluorescent detection (FLD) method to quantify hIgG in solution.
296 Analysis of human IgG in solution (0.1 mg/mL) showed two peaks (Figure 1A): the first one
297 corresponds to a dimeric form of hIgG (~8.2 min) and the second to the monomeric hIgG (~9.2
298 min). As the first peak area was very small compared to ~~that of~~ the 2nd one (peak area ratio: ~8),
299 dimeric hIgG was not considered for hIgG calibration. Repeatability and intermediate precision
300 of SEC-FLD method have been evaluated. The intra (n=3) and inter-day (n=3) RSD of the
301 retention times (Tr) were less than 0.1%. Resolution and limit of quantification were also
302 evaluated at 1.3 and 160 nM respectively (see Supplementary Material, method validation
303 chapter).

304 Considering the antibodies grafting density, it is important to note that for each type of beads,
305 the grafting protocol differs in terms of buffers (i.e. pH and ionic strength) thermal and/or
306 agitation that may impact protein conformation and thereby fluorescent intensities measured.
307 Therefore, hIgG free in solution (0.1 mg/mL) were submitted to experimental conditions

308 mimicking the grafting protocols applied to COOH and Ts beads. The agitation used for hIgG
309 grafting on COOH beads (rotating wheel at 4 °C overnight) led to a slight decrease of the FLD
310 signal (-5,2 %) compared to the reference sample of hIgG (PBS at 4 °C). The FLD signal further
311 decrease (19%) when EDC and Sulfo-NHS were added in the reaction medium. To explain this
312 decrease, we hypothesized that the temperature (4 °C) as well as EDC and Sulfo-NHS could
313 increase the intra amino acids interactions favoring thereby conformation where fluorescent
314 amino acids are hindered. For Ts beads, an increase of the FLD signal (+9,6 %) was observed
315 with the Ts grafting protocol (stirring at 37 °C during 16h). This signal is increased by 18 %
316 when Ts conjugation protocol is performed in borate buffer pH 9.5 (Figure 1B). The increase
317 of the fluorescent signal could be related to a partial denaturation of the hIgG. Several studies
318 have demonstrated that thermally induced unfolding of proteins led to the exposure of the
319 fluorescent amino previously buried (e.g. tryptophan) increasing thereby the fluorescent signal
320 [26]. The same type of experiments has been performed for hIgG cleaved by IdeS. Digested
321 IgG (0.22 mg/mL) has been first analyzed with SEC-FLD, showing two peaks: 1st peak (~9.99
322 min) corresponding to Fab₂ fragment of 100 kDa; 2nd peak (~10,98 min) to Fc one (50 kDa)
323 (Figure 2). Four calibration curves of hIgG cleaved by *IdeS* into Fab₂ (~100 kDa) and Fc (~50
324 kDa) fragments have been performed under the grafting conditions selected for the 4 types of
325 beads (figure 3). A variation has been observed for Fc peaks: a 25% decrease of the curve's
326 slope for COOH beads conditions compared to Ts beads which could lead to underestimate an
327 unfavorable orientation (see Figure 3A and B). Therefore, we can conclude from these results
328 that calibration curves of hIgG and its fragments have to be established for each type of beads
329 studied (i.e. COOH, Ts, streptavidin, protein G) to evaluate accurately the antibodies grafting
330 density and orientation.

331

332 **3.2. Antibodies grafting density and orientation on magnetic microbeads**

333 We then evaluated the grafting density and hIgG orientation on the four types of beads:
334 carboxylated, tosylated, protein G and streptavidin. For this purpose, magnetic beads bearing
335 hIgG have been digested by *IdeS* and the fragments released analyzed by SEC-FLD.

336

337 3.2.1. *F(ab)₂* and *Fc* quantitation.

338 We first verified that *IdeS* did not overlap with peaks corresponding to hIgG fragments in our
339 experimental conditions by analysing *IdeS* (5 U) as a control. Indeed, molecular weight of *IdeS*
340 is approximately 37 kDa which might interfere with hIgG fragments detection. For *IdeS*, two
341 peaks were observed at 10.08 min (dimer) and 11.0 min (monomer) with retention times close
342 to *F(ab)₂* and *Fc* ones which could lead to overestimate peak areas related to *Fc* and, into a lesser
343 extent, to *Fab₂* (see Figure S1 in Electronic Supplementary Material). Therefore, to accurately
344 quantify the amount of *F(ab)₂* and *Fc* released after the digestion of hIgG grafted on magnetic
345 beads, a calibration curve for *IdeS* (from 1 U to 14 U) was drawn using different injection
346 volumes (see Fig S2, Electronic Supplementary Material) and was used to evaluate the contribution of *IdeS*
347 contribution in *Fab₂* and *Fc* peak areas values. Therefore, peak areas of *F(ab)₂* and *Fc* fragments
348 were corrected with *IdeS* calibration in the whole study allowing a more accurate quantification
349 (see Table S1, Supplementary material).

350

351 3.2.2. Grafting density and hIgG orientation on the different types of beads

352 To estimate the percentage of hIgG grafted (%), washing fractions and supernatants were
353 analyzed and Equation 1 was used to estimate this value:

$$354 \quad \%_{grafted} = \frac{m_i - (m_{washing} + m_{supernatant})}{m_i} \quad Eq. 1$$

355

356 where m_i is the initial quantity of hIgG per mg of beads before grafting, $m_{washing}$ and $m_{supernatant}$
357 are the quantity of hIgG found after the grafting step in washing solutions and supernatants

358 respectively. A calibration curve of non-digested hIgG in solution in PBS was performed to
359 quantify remaining hIgG in the supernatant and washing solution (see Figure S2 in
360 Supplementary Material).

361 From the percentage values evaluated for the different beads (Figure 4A), we can conclude that
362 protein G beads can graft more IgG than other beads (95.1% of injected IgG are grafted), with
363 COOH beads being the less efficient with a lower density of IgG grafted on their surface
364 (73.8%).

365 The number of hIgG per bead has been also evaluated by considering the average mass of an
366 hIgG (150 kDa), the bead's density (1.8 g/cm³ for Ts, COOH and streptavidin beads, 2.0 g/cm³
367 for protein G beads) and average diameter of the beads (1 μm), using the following equation:

$$368 \quad \text{Number of IgG molecules per bead} = \frac{\%_{\text{grafted}} \times m_i}{m_{\text{IgG}}} \times \frac{m_{\text{bead}}}{1 \text{ mg of beads}} \quad (\text{Eq.2})$$

369 where %_{grafted} is the proportion of grafted hIgG on the beads, m_i the initial mass (μg) of hIgG
370 incubated with 1 mg of beads for grafting, m_{IgG} the mass (μg) of one hIgG molecule, m_{bead} the
371 mass (μg) of the corresponding bead.

372 According to Figure 4B, protein G beads grafted a high number of hIgG (~70 000 molecules
373 per bead), followed by Ts beads (~56 000 IgG molecules per bead), streptavidin beads (~25 000
374 molecules) and finally COOH ones (~12 000). We can note that despite a higher quantity of
375 hIgG employed for carboxylic beads (79 μg) compared to protein G (49.91 μg) the amount of
376 hIgG grafted is better for proteins G beads. The same observation can be made for Ts beads,
377 where better grafting compared to carboxylic beads is observed despite the smaller
378 concentration of hIgG used (39,6 μg). These results suggest that the grafting efficiency is not
379 only related to the amount of hIgG in the immobilization solution but also to the surface
380 chemistry.

381

382 The hIgG orientation has been evaluated by *IdeS* digestion and the analysis of released
383 fragments. Figure 5A displays the different chromatograms obtained for COOH, Ts,
384 streptavidin and protein G beads. The peak areas and notably Fab₂/Fc ratio highlighted the
385 differences between beads in terms of number of hIgG grafted and hIgG orientations. From
386 Figure 5A, we have observed that protein G beads lead to a larger peak of F(ab)₂ compared to
387 other beads. The orientation ratio (Fab₂/(Fab₂+Fc)) showed that protein G beads also exhibit the
388 best orientation (~73.8% of antibodies grafted by their Fc fragment) (Figure 5B) compared to
389 Ts (31.3%), streptavidin (9.9%) and carboxylic beads (5.2%). We can conclude from these
390 results that protein G led not only to more grafted antibodies but also to a higher proportion of
391 well orientated immobilized hIgG. This could be due to the surface chemistry of carboxylic and
392 Ts beads that led to a random immobilization of hIgG via amino (carboxylic and Ts) and
393 sulfhydryl groups (Ts). Therefore, only a fraction of the F(ab)₂ binding sites will be potentially
394 available for biorecognition. The better orientation ratio observed for Ts compared to carboxylic
395 beads could be related to the hydrophobic surface of tosyl beads favoring hIgG orientation
396 through the more hydrophobic Fc region. In contrast, for protein G, immobilization through Fc
397 fragment allow a better orientation with a higher proportion of F(ab)₂ available.

398

399 *IdeS* digestion efficiency on the magnetic beads

400 To ensure that the better peak area ratio Fab₂/Fc observed in Protein G was related to a better
401 orientation and not to a higher enzymatic digestion efficiency, *IdeS* digestion yield has been
402 estimated (Equation 3).

$$403 \quad \%_{digested} = \frac{m_{digested}}{m_i - (m_{washing} + m_{supernatant})} \quad Eq. 3$$

404 Digestion efficiency %_{digested} introduced in Eq.3 is directly correlated to biologically
405 available hIgG, where m_i is the initial quantity of hIgG per mg of beads before grafting, m_{washing}

406 and $m_{\text{supernatant}}$ are the quantity of hIgG found in washing liquids and supernatants and m_{digested}
407 is the quantity of hIgG found in the digestate after IdeS digestion.

408 Indeed, we considered that *IdeS* cannot fully digest every hIgG molecule grafted on the
409 bead, which means that this method could give an underestimated quantification of hIgG
410 available to *IdeS* molecules. Being a relatively large molecule (~37kDa), *IdeS* may not access
411 easily to the hinge region of some hIgG molecules within the antibody layers (or multilayers),
412 resulting in a partial proteolysis yield. Assuming that these unavailable hIgG molecules would
413 not be available for other reactions with biomolecules (such as antigen recognition and capture),
414 we can suppose that the digestion yield also reflects the antigen capture potential of the beads.
415 The results showed that *IdeS* digestion yield is higher for tosylactivated beads (46.3%) than
416 protein G (34,2%) and streptavidin (37,5%). Unexpectedly, we found a very low digestion yield
417 for COOH beads (5.6%), as depicted in Figure 6.

418 The lower digestion yield for protein G beads compared to the tosylactivated beads is probably
419 related to the higher grafting density leading thereby to a steric hindrance detrimental for *IdeS*
420 biological activity. Considering the better ratio $\text{Fab}_2/(\text{Fab}_2+\text{Fc})$ and the lower digestion yield of
421 IdeS for protein G beads, these results confirm the better orientation of hIgG on this kind of
422 beads.

423 Therefore, the overall results showed that protein G beads exhibit the best orientation
424 ratio as well as the best grafting density. This could be explained by their ability to capture hIgG
425 through Fc fragment, leading thereby to a more favorable orientation [27]. In contrast, hIgG are
426 randomly immobilized by covalent bonding for COOH and Ts beads and via Biotin interactions
427 (non-covalent) for Streptavidin beads [28]. In addition, Streptavidin beads rely on a
428 biotinylation procedure prior to antibody grafting on beads. This additional step may decrease
429 the efficiency of the whole conjugation procedure as biotinylation will not be total. Finally,
430 protein G beads offer the best results in terms of antibody orientation and density on the surface.

431 Moreover, they are particularly easy to graft with ~1h30 to complete the whole procedure
432 compared to 18h for Ts and 30h for COOH beads, which makes them the best candidate for
433 antibody grafting and immunocapture.

434 Concerning ProtA/ProtG beads, these results are in agreement with *Shen et al* [17] in
435 terms of antibody coverage and orientation ratio. In contrast, for carboxylated beads, a high
436 difference is observed with our study. This discrepancy could be related to the digestion tool
437 employed. Indeed, with trypsin digestion, employed by *Shen et al.*, the peptides released from
438 the F(ab)₂ region, detected and quantified by LC-MS, could arise from antibodies attached on
439 beads via one Fab fragment. This could lead therefore to an overestimation of the orientation
440 ratio for COOH beads where antibodies are randomly immobilized. On Prot G/A beads, where
441 antibodies are immobilized via Fc fragments and thereby well oriented. Our method combining
442 IdeS digestion with SEC analysis offers size discrimination making it possible to retrieve more
443 information to identify the fragment released (i.e. Fc (50 kDa) vs F(ab)₂ (100 kDa).

444 We have therefore developed a direct accurate and rapid quantification method of
445 bioavailable hIgG on magnetic beads. Our study takes into account beads grafting conditions
446 and *IdeS* contribution effect on FLD signal and absorption on beads for a more accurate
447 quantification. Finally, we compared the performance of COOH, Ts and protein G beads for
448 capturing TNF- α , a cytokine involved in Major Depressive Disorders (MDD) and other
449 inflammatory-related pathologies. Streptavidin beads were not considered in the study as they
450 did not provide added value compared to carboxylated and tosylactivated beads.

451

452 **3.3. Application for immunocapture of TNF- α : towards quantification of biomarkers in** 453 **biological fluids**

454 To illustrate the performance of the previously studied magnetic beads, COOH, Ts and
455 protein G beads were grafted with monoclonal anti-human-TNF- α antibodies following the

456 procedure previously described. 5 ng of human TNF- α were then incubated for 4 hours at 25
457 °C with 100 μ g of grafted magnetic beads of each type. Elution of antigens was done using
458 thermal elution in PBS at 95°C for 5 minutes in order to maximize the amount of antigen release
459 and minimize protein denaturation [29]. Eluates were then prepared in three dilutions: non
460 diluted, ten and one hundredfold diluted to ensure that recovered antigen concentration matched
461 the immunoassay's linear range. Quantification was carried out using an ELISA kit for human
462 TNF- α on microplate by absorbance spectrometry. A calibration curve was built using human
463 TNF- α standard solution. The standard was also treated at 95°C for 5 minutes in order to reflect
464 possible conformational changes of TNF- α that would affect immunoassay detection. As shown
465 in Figure S3, thermal treatment influenced calibration curve slope with a 40% decrease in slope
466 after thermal treatment. Quantification of eluates from the beads was therefore performed using
467 the thermal treatment calibration curve. Results are shown in Table 1.

468 For 5.0 ng of human TNF- α incubated with 100 μ g of beads, 67.6% of TNF- α was recovered
469 with protein G beads, but only 6.6% and 2.8% for COOH and Ts beads respectively. These
470 results support the high antibody grafting efficiency of protein G beads in terms of both
471 antibody coverage and orientation. For COOH and Ts beads, they suggest a very low capture
472 ability of these beads for this application probably due to poor orientation and/or antibody
473 density. However, it should be noted that thermal elution does not necessarily elute all the
474 captured antigens. Nevertheless, it is still the mildest procedure for antigen elution without
475 causing full protein denaturation (from acidic media) that would render accurate quantification
476 with ELISA impossible. These results are in agreement with our SEC FLD study highlighting
477 the better grafting and orientation of hIgG on protein G magnetic beads. They are therefore
478 promising candidates for sensitive and specific detection of biomarkers like TNF- α and could
479 be extended to other cytokines or proteins.

480

481
482
483
484
485
486
487
488
489
490
491
492
493
494
495
496
497
498

4. Conclusion

In the present study, we present an original analytical method for the evaluation of human IgG grafting efficiency on 4 types of commercial magnetic beads for immunocapture applications. This method relies on an innovative combination of a highly specific digestion of hIgG by IdeS together with the high resolution of the fragments' analysis by SEC, offering an efficient determination of antibodies orientation. This work offers a comprehensive approach of the influence of grafting conditions, *IdeS* and bead's surface chemistry on fluorescent signal detection. All results support the high efficiency of protein G magnetic beads for a high grafting yield of human IgG (~70 000 IgG molecules per bead) and an optimal orientation of antibodies for antigen capture (75% of Fab₂ fragment free). Moreover, protein G beads ease-of-use in terms of grafting conditions and time make them a powerful and convenient tool for biosensing and lab-on-a-chip applications. These findings have been illustrated with a high-value application for the immunocapture and elution of human TNF- α at 20 ng/mL, towards the monitoring of inflammatory-related pathologies. This work will be extended to other cytokines. Finally, this method can be more generally used to assess the hIgG coverage and orientation on any type of surface, relying on the high specificity and efficiency of the *IdeS* digestion of hIgG.

499 **REFERENCES**

- 500
- 501 1. Hou Z, Liu Y, Xu J, Zhu J (2020) Surface engineering of magnetic iron oxide
- 502 nanoparticles by polymer grafting: Synthesis progress and biomedical applications.
- 503 *Nanoscale* 12:14957–14975
- 504 2. Kruszewska J, Zajda J, Matczuk M (2021) How to effectively prepare a sample for
- 505 bottom-up proteomic analysis of nanoparticle protein corona? A critical review. *Talanta*
- 506 226
- 507 3. Khizar S, Ben Halima H, Ahmad NM, Zine N, Errachid A, Elaissari A (2020) Magnetic
- 508 nanoparticles in microfluidic and sensing: From transport to detection. *Electrophoresis*
- 509 41:1206–1224
- 510 4. Liu S, Haller E, Horak J, Brandstetter M, Heuser T, Lämmerhofer M (2019) Protein A-
- 511 and Protein G-gold nanoparticle bioconjugates as nano-immunoaffinity platform for
- 512 human IgG depletion in plasma and antibody extraction from cell culture supernatant.
- 513 *Talanta* 194:664–672 . <https://doi.org/10.1016/j.talanta.2018.10.079>
- 514 5. Zhang L, Hu D, Salmain M, Liedberg B, Boujday S (2019) Direct quantification of
- 515 surface coverage of antibody in IgG-Gold nanoparticles conjugates. *Talanta* 204:875–
- 516 881 . <https://doi.org/10.1016/j.talanta.2019.05.104>
- 517 6. Kozłowski R, Ragupathi A, Dyer RB (2018) Characterizing the Surface Coverage of
- 518 Protein-Gold Nanoparticle Bioconjugates. *Bioconjug Chem* 29:2691–2700 .
- 519 <https://doi.org/10.1021/acs.bioconjchem.8b00366>
- 520 7. Walkey CD, Olsen JB, Guo H, Emili A, Chan WCW (2012) Nanoparticle size and
- 521 surface chemistry determine serum protein adsorption and macrophage uptake. *J Am*
- 522 *Chem Soc* 134:2139–2147 . <https://doi.org/10.1021/ja2084338>
- 523 8. Hinterwirth H, Lindner W, Lämmerhofer M (2012) Bioconjugation of trypsin onto gold
- 524 nanoparticles: Effect of surface chemistry on bioactivity. *Anal Chim Acta* 733:90–97 .

- 525 <https://doi.org/10.1016/j.aca.2012.04.036>
- 526 9. Young MB, Oh BK, Lee W, Won HL, Choi JW (2005) Study on orientation of
527 immunoglobulin G on protein G layer. *Biosens Bioelectron* 21:103–110 .
528 <https://doi.org/10.1016/j.bios.2004.09.003>
- 529 10. Song HY, Zhou X, Hogley J, Su X (2012) Comparative study of random and oriented
530 antibody immobilization as measured by dual polarization interferometry and surface
531 plasmon resonance spectroscopy. *Langmuir* 28:997–1004 .
532 <https://doi.org/10.1021/la202734f>
- 533 11. Yoshimoto K, Nishio M, Sugawara H, Nagasaki Y (2010) Direct observation of
534 adsorption-induced inactivation of antibody fragments surrounded by mixed-PEG layer
535 on a gold surface. *J Am Chem Soc* 132:7982–7989 . <https://doi.org/10.1021/ja910372e>
- 536 12. Fujiwara K, Watarai H, Itoh H, Nakahama E, Ogawa N (2006) Measurement of
537 antibody binding to protein immobilized on gold nanoparticles by localized surface
538 plasmon spectroscopy. *Anal Bioanal Chem* 386:639–644 .
539 <https://doi.org/10.1007/s00216-006-0559-2>
- 540 13. Liu S, Horak J, Höldrich M, Lämmerhofer M (2017) Accurate and reliable
541 quantification of the protein surface coverage on protein-functionalized nanoparticles.
542 *Anal Chim Acta* 989:29–37 . <https://doi.org/10.1016/j.aca.2017.08.004>
- 543 14. Bouzas-Ramos D, Trapiella-Alfonso L, Pons K, Encinar JR, Costa-Fernández JM,
544 Tsatsaris V, Gagey-Eilstein N (2018) Controlling Ligand Surface Density on
545 Streptavidin-Magnetic Particles by a Simple, Rapid, and Reliable Chemiluminescent
546 Test. *Bioconjug Chem* 29:2646–2653 .
547 <https://doi.org/10.1021/acs.bioconjchem.8b00347>
- 548 15. Näreoja T, Ebner A, Gruber HJ, Taskinen B, Kienberger F, Hänninen PE, Hytönen VP,
549 Hinterdorfer P, Härmä H (2014) Kinetics of bioconjugate nanoparticle label binding in

- 550 a sandwich-type immunoassay. *Anal Bioanal Chem* 406:493–503 .
551 <https://doi.org/10.1007/s00216-013-7474-0>
- 552 16. Hua X, You H, Luo P, Tao Z, Chen H, Liu F, Wang M (2017) Upconversion
553 fluorescence immunoassay for imidaclothiz by magnetic nanoparticle separation. *Anal*
554 *Bioanal Chem* 409:6885–6892 . <https://doi.org/10.1007/s00216-017-0653-7>
- 555 17. Shen M, Jiang D, De Silva PIT, Song B, Rusling JF (2019) Restricted Proteolysis and
556 LC-MS/MS to Evaluate the Orientation of Surface-Immobilized Antibodies. *Anal*
557 *Chem* 91:4913–4919 . <https://doi.org/10.1021/acs.analchem.9b01155>
- 558 18. Johansson BP, Shannon O, Björck L (2008) IdeS: A bacterial proteolytic enzyme with
559 therapeutic potential. *PLoS One* 3: . <https://doi.org/10.1371/journal.pone.0001692>
- 560 19. Sasso LA, Aran K, Guan Y, Ündar A, Zahn JD (2013) Continuous Monitoring of
561 Inflammation Biomarkers During Simulated Cardiopulmonary Bypass Using a
562 Microfluidic Immunoassay Device-A Pilot Study. *Artif Organs* 37: .
563 <https://doi.org/10.1111/aor.12021>
- 564 20. Kumar S, Tripathy S, Jyoti A, Singh SG (2019) Recent advances in biosensors for
565 diagnosis and detection of sepsis: A comprehensive review. *Biosens. Bioelectron.* 124–
566 125:205–215
- 567 21. Yndestad A, Damås JK, Øie E, Ueland T, Gullestad L, Aukrust P (2006) Systemic
568 inflammation in heart failure - The whys and wherefores. *Heart Fail. Rev.* 11:83–92
- 569 22. Russell B, Moss C, George G, Santaolalla A, Cope A, Papa S, Van Hemelrijck M
570 (2020) Associations between immune-suppressive and stimulating drugs and novel
571 COVID-19—a systematic review of current evidence. *Ecancermedicalsecience* 14: .
572 <https://doi.org/10.3332/ecancer.2020.1022>
- 573 23. Mehta P, McAuley DF, Brown M, Sanchez E, Tattersall RS, Manson JJ (2020)
574 COVID-19: consider cytokine storm syndromes and immunosuppression. *Lancet*

- 575 395:1033–1034
- 576 24. Slavich GM, Irwin MR (2014) From stress to inflammation and major depressive
577 disorder: A social signal transduction theory of depression. *Psychol Bull* 140:774–815 .
578 <https://doi.org/10.1037/a0035302>
- 579 25. Cizza G, Marques AH, Eskandari F, Christie IC, Torvik S, Silverman MN, Phillips
580 TM, Sternberg EM (2008) Elevated Neuroimmune Biomarkers in Sweat Patches and
581 Plasma of Premenopausal Women with Major Depressive Disorder in Remission: The
582 POWER Study. *Biol Psychiatry* 64:907–911 .
583 <https://doi.org/10.1016/j.biopsych.2008.05.035>
- 584 26. Brader ML, Estey T, Bai S, Alston RW, Lucas KK, Lantz S, Landsman P, Maloney
585 KM (2015) Examination of thermal unfolding and aggregation profiles of a series of
586 developable therapeutic monoclonal antibodies. *Mol Pharm* 12:1005–1017 .
587 <https://doi.org/10.1021/mp400666b>
- 588 27. Choe W, Durgannavar TA, Chung SJ (2016) Fc-binding ligands of immunoglobulin G:
589 An overview of high affinity proteins and peptides. *Materials (Basel)*. 9
- 590 28. Foddai A, Elliott CT, Grant IR (2010) Maximizing capture efficiency and specificity of
591 magnetic separation for mycobacterium avium subsp. paratuberculosis cells. *Appl*
592 *Environ Microbiol* 76:7550–7558 . <https://doi.org/10.1128/AEM.01432-10>
- 593 29. Mai TD, Pereiro I, Hiraoui M, Viovy JL, Descroix S, Taverna M, Smadja C (2015)
594 Magneto-immunocapture with on-bead fluorescent labeling of amyloid- β peptides:
595 towards a microfluidized-bed-based operation. *Analyst* 140:5891–5900 .
596 <https://doi.org/10.1039/c5an01179e>
- 597
- 598
- 599

600 **Figures captions**

601 **Fig. 1** Analysis of hIgG (0.1 mg/mL) by SEC-FLD: (A) control sample (human IgG in PBS at
602 4°C), (B) Influence of bead grafting conditions on FLD signal of human IgG. COOH
603 conditions are agitation at 20 rpm on rotating wheel at 4°C overnight in PBS, with 10 mg/mL
604 of EDC and Sulfo-NHS. Ts conditions are agitation a 650 rpm on Thermomixer at 37°C for
605 16h with borate and ammonium buffer pH 9.5.
606 Mobile phase was 50 mM sodium phosphate, 150 mM NaCl and 10% isopropanol pH 6.5.
607 Column: BioSEC-3, (4.6 mm × 300 mm, 300 Å, particle diameter 3 µm); Flow rate:
608 300 µL/min; FLD: λ_{ex} =280 nm, λ_{em} =340 nm

609
610 **Fig. 2** SEC-FLD analysis of human IgG at 0.22 mg/mL in PBS after IdeS digestion.
611 Experimental conditions as mentioned in Figure 1

612
613 **Fig. 3** Calibration curves corresponding to grafting conditions, A) Fab₂ fragment, B) Fc
614 fragment. Experimental conditions as mentioned in Figure 1

615
616 **Fig. 4** hIgG immobilization study on beads: (A) grafting efficiency, (B) number of hIgG
617 molecules per bead

618
619 **Fig. 5** IdeS digestion of Immobilized hIgG: **A)** SEC – FLD Analysis,
620 **B)** Evaluation of the percentage of hIgG orientated with F(ab)₂ free on the beads surface.

621 Experimental conditions as Figure 1

622
623 **Fig. 6** Comparison of IdeS digestion efficiency for COOH, Ts, Streptavidin and Protein G
624 magnetic beads

625

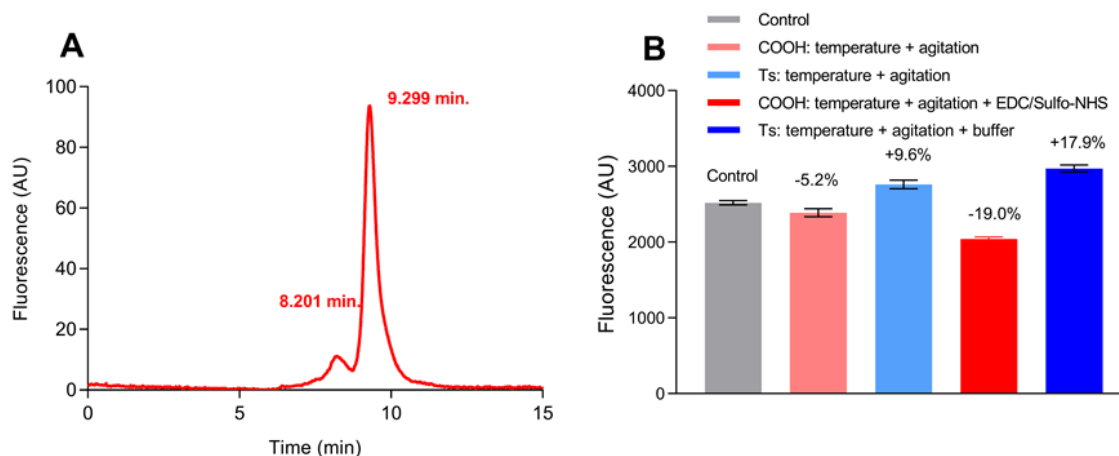
626 **Table 1** Comparison of beads efficiency for immunocapture of TNF- α (n=5 replicates per

627 bead)

628

629

630



631 **Fig. 1** Analysis of hIgG (0.1 mg/mL) by SEC-FLD: (A) control sample (human IgG in PBS at
632 4°C), (B) Influence of bead grafting conditions on FLD signal of human IgG. COOH
633 conditions are agitation at 20 rpm on rotating wheel at 4°C overnight in PBS, with 10 mg/mL
634 of EDC and Sulfo-NHS. Ts conditions are agitation a 650 rpm on Thermomixer at 37°C for
635 16h with borate and ammonium buffer pH 9.5.
636 Mobile phase was 50 mM sodium phosphate, 150 mM NaCl and 10% isopropanol pH 6.5.
637 Column: BioSEC-3, (4.6 mm × 300 mm, 300 Å, particle diameter 3 μm); Flow rate:
638 300 μL/min; FLD: λ_{ex} =280 nm, λ_{em} =340 nm
639

640

641

642

643

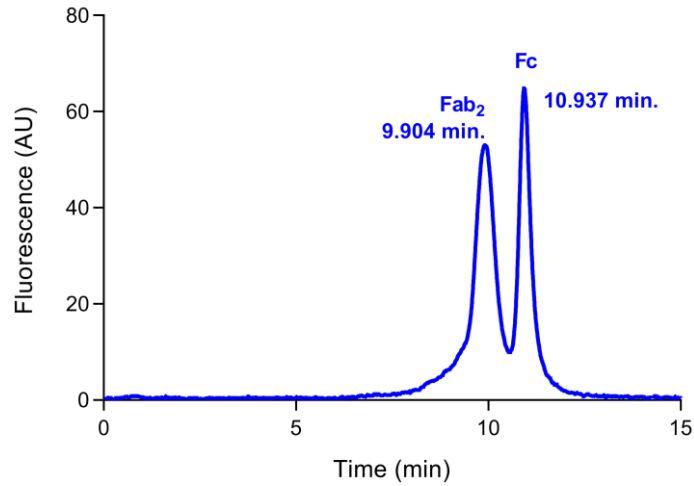
644

645

646

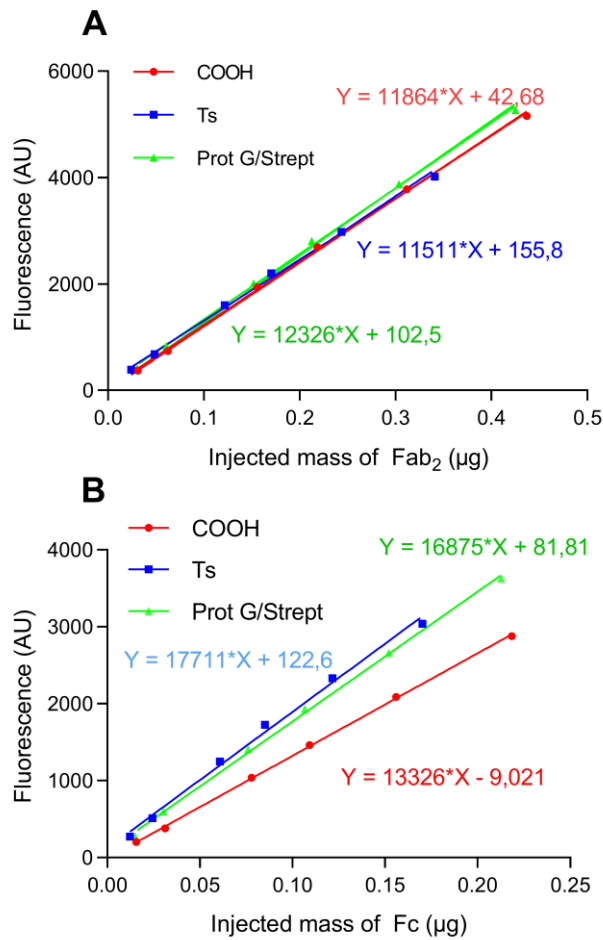
647

648



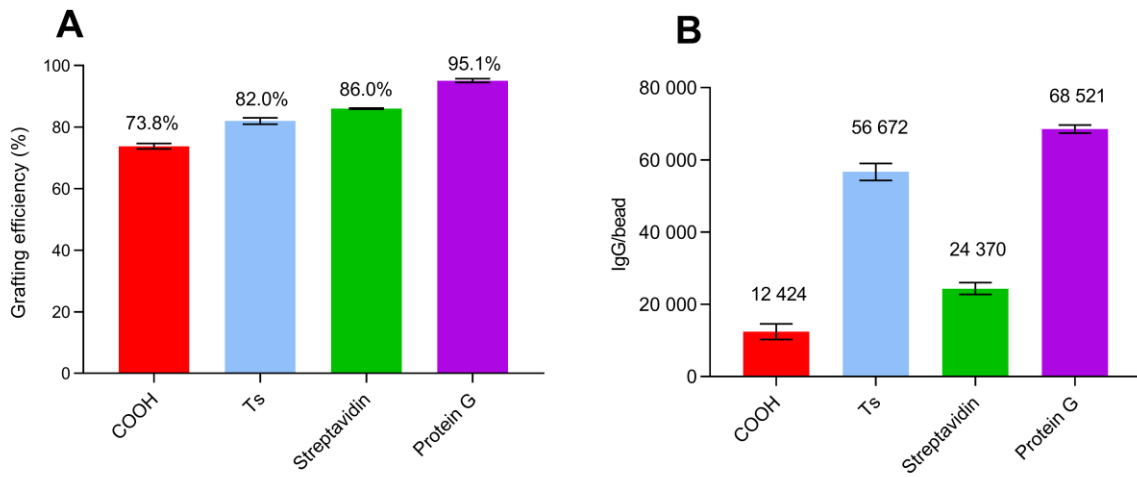
649
650
651
652
653

Fig. 2 SEC-FLD analysis of human IgG at 0.22 mg/mL in PBS after IdeS digestion. Experimental conditions as mentioned in Figure 1



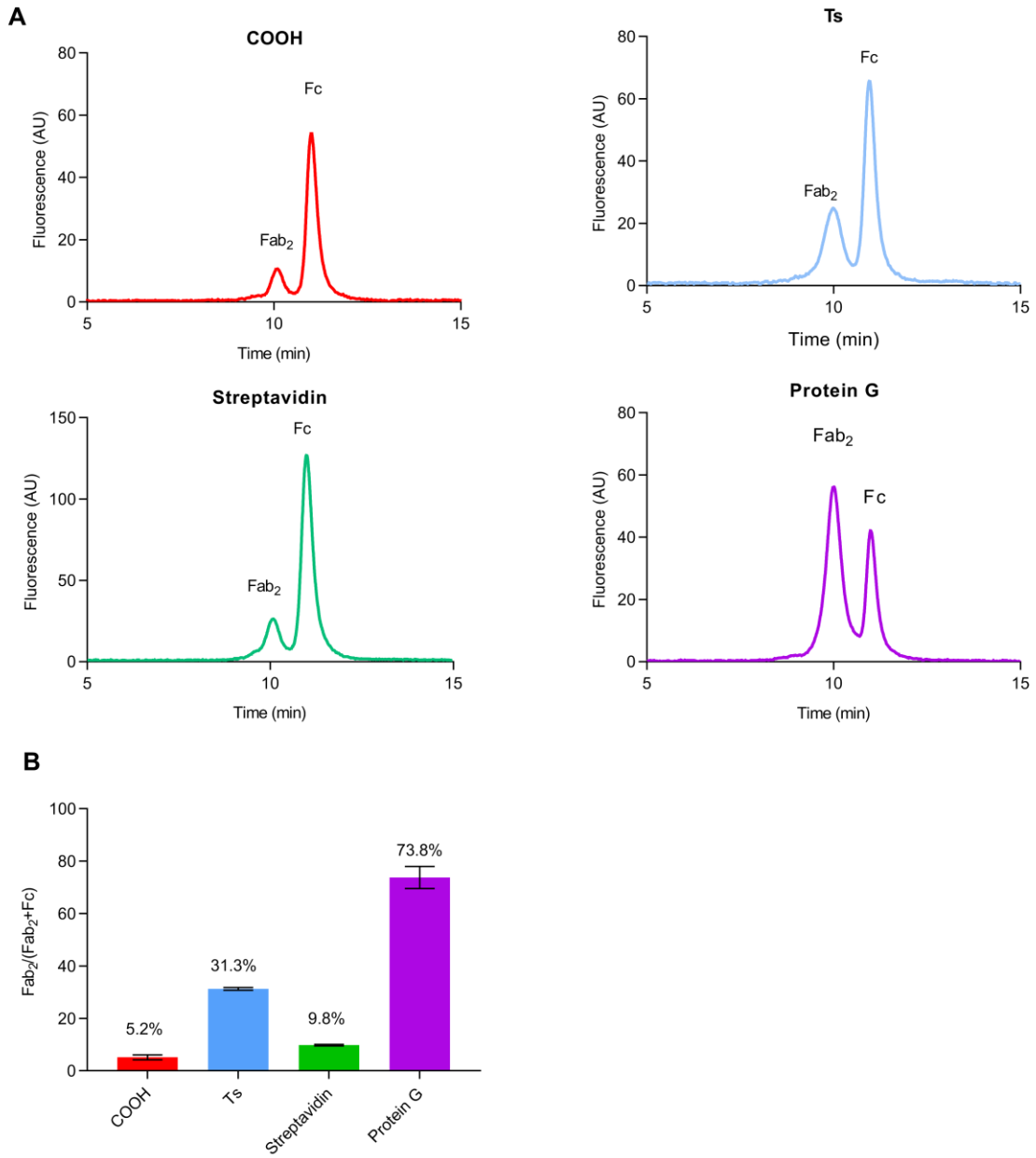
654
655
656
657
658

Fig. 3 Calibration curves corresponding to grafting conditions: A) Fab₂ fragment, B) Fc fragment. Experimental conditions as mentioned in Figure 1



659
660
661
662
663

Fig. 4 hIgG immobilization study on beads: (A) grafting efficiency, (B) number of hIgG molecules per bead



664 **Fig. 5** IdeS digestion of Immobilized hIgG: **A)** SEC – FLD Analysis,
665 **B)** Evaluation of the percentage of hIgG orientated with F(ab)₂ free on the beads surface.
666 Experimental conditions as Figure 1
667
668

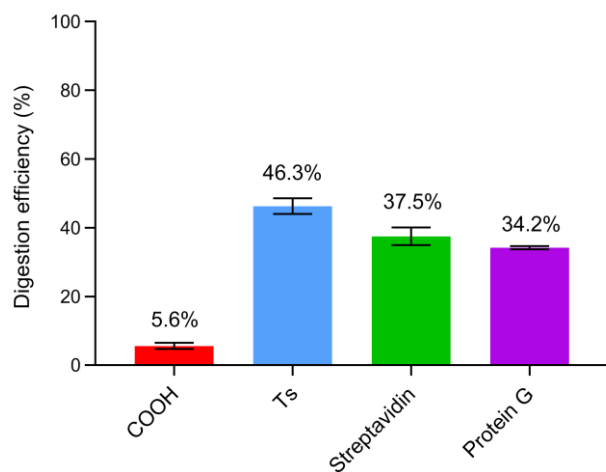
669

670

671

672

673



674

675 **Fig. 6** Comparison of IdeS digestion efficiency for COOH, Ts, Streptavidin and Protein G
676 magnetic beads

677

	COOH beads	Ts beads	Protein G beads
<i>TNF-α recovered after thermal elution (% RSD) (ng/100 μg of beads)</i>	0.33 (15%)	0.14 (13%)	3.38 (17%)

678

679 **Table 1** Comparison of beads efficiency for immunocapture of TNF-α (n=5 replicates per
680 bead)

681